ISSN 1063-7842, Technical Physics, 2016, Vol. 61, No. 12, pp. 1789–1796. © Pleiades Publishing, Ltd., 2016.
Original Russian Text © G.T. Aldoshin, S.P. Yakovlev, 2016, published in Zhurnal Tekhnicheskoi Fiziki, 2016, Vol. 86, No. 12, pp. 25–32.

ATOMIC AND MOLECULAR PHYSICS

Mechanical Model of Carbon Dioxide Vibrational Spectrum

G. T. Aldoshin and S. P. Yakovlev*

Ustinov Baltic State Technical University VOENMEKh,
Pervaya Krasnoarmeiskaya ul. 1, St. Petersburg, 190005 Russia
**e-mail: yakovlev_sp@mail.ru*

Received November 23, 2015; in final form, May 10, 2016

Abstract—Classical dynamics methods have been used to study the nonlinear vibrations of a CO_2 molecule. Consideration includes not only the anharmonicity valence angle, which enables one to explain the Fermi resonance, but also the physical nonlinearity of the force field (stiffness and softness of springs). In the farthest neighbor approximation (with regard to oxygen–oxygen interaction), a set of nonlinear differential equations in the Lagrangian form has been derived. Their analytical solution has been derived using the method of invariant normalization. The occurrence of a strange attractor has been discovered by numerical simulation. Recommendations for the selection of initial conditions are given that take into account the possibility of regular beatings that change into to chaotic beatings.

DOI: 10.1134/S1063784216120033

INTRODUCTION

In the gaseous (vapor) state, molecules are disordered and move independently, except for instants of collisions. The translational and vibrational motions of molecules, as well as the vibrations of atoms inside them, can be considered to be unaffected by other molecules. Therefore, the behavior of individual molecules is of primary interest in studying the gaseous state.

Classical (Newtonian) mechanics has long been widely used in the kinetic theory of gases. However, it is generally accepted that the range of applicability of classical mechanics is limited by sizes that are not too small. Nevertheless, the laws of classical mechanics work even on the interatomic distance scale. The notion of the *point mass* as an object that possesses an inertial mass, is devoid of an internal structure and has sizes that are much smaller than the characteristic sizes of a given problem is not defined quantitatively. As a result, atomic nuclei, which are much heavier than electrons, can be considered as classical point masses in many problems. A molecule is viewed as a dynamic system that has a constant composition, i.e., a constant number of bonded atoms (bonds are simulated by weightless springs) that oscillate about an equilibrium configuration. Newton's third law imposes restrictions on forces with which two particles act on each other; i.e., the forces must be oppositely directed along a straight line that passes through the particles and have the same value. This law ignores electrodynamic interactions, except for Coulomb attraction and repulsion. Therefore, only static forces, i.e., those that depend on the mutual arrangement of point masses can be considered. Thus, in keeping within the Newton, Lagrangian, and Hamilton principles, classical mechanics allows us to study and explain mechanical vibrations of atoms in a molecule.

The theory of small-amplitude linear vibrations was developed long ago [1, 2]. In the linear approximation, only the most intense spectral lines are studied. The introduction of geometrical nonlinearity (valence angle anharmonicity) [3] dramatically changes the motion pattern; namely, a strong interaction arises between oscillation modes, which is accompanied by a periodic energy exchange (transfer) between these modes and the spitting of the Raman fundamental frequency. This phenomenon, which was discovered by Rosetti in 1931 and explained by Fermi [4] in the same year, is known as the Fermi resonance.

It is natural to expect new effects in the vibrations of a molecule if additional sources of anharmonicity appear in its mechanical model. These are, specifically, the interaction of oxygen atoms with each other (farthest neighbor approximation) and the physical nonlinearity of the CO_2 force field (stiffness or softness of springs) [5].

1. DEFINITION OF THE PROBLEM AND BASIC EQUATIONS

We consider the free vibrations of a CO_2 molecule. The computational model of the problem and main designations are presented below.

(i) m_C and m_O are the masses of C and O atoms, respectively, as point masses.

(ii) O(x_1, y_1, 0), C(x_2, y_2, 0), and O(x_3, y_3, 0) are the current positions of the atoms.

(iii) ν_1 is the linearized eigenfrequency corresponding to vibrations ϑ_1 that are symmetric about the center of mass of the molecule, ν_2 is the frequency of deformation or flexural vibrations ϑ_2 of the molecule, and ν_3 is the frequency of antisymmetric or skew-symmetric vibrations ϑ_3 of the molecule (see [3]).

In contrast to [3], the given model takes into account that the forces of oxygen–carbon and oxygen–oxygen interaction are nonlinear.

(iv) f_{CO} is the linear part of the stiffness of a weightless spring that simulates the C–O interatomic bonds (valence stiffness), $f_1(\Delta l_{ij}, \varphi)$ is the nonlinear component of the stiffness, Δl_{ij} is the change in the distance between the ith and jth atoms ($i \neq j$), and φ is the change in the valence angle OCO.

(v) f_{OO} is the linear part of the stiffness of a spring that simulates interaction between the farthest neighbors, and $f_2(\Delta l_{ij}, \varphi)$ is its nonlinear component.

(vi) $(f_{\varphi\varphi} + f_3(\Delta l_{ij}, \varphi))$ is the deformation (flexural) stiffness (correction coefficients are taken according to experimental data in [5]).

The dimensionless Hamiltonian of the system in normal coordinates $\bar{\vartheta}_1 = (\bar{x}_3 - \bar{x}_1)/2$ (symmetric), $\bar{\vartheta}_2 = \bar{y}_1$ (deformational), and $\bar{\vartheta}_3 = (\bar{x}_1 + \bar{x}_3)/2$ (antisymmetric) has the form (here, $\bar{x}_1 = (x_1 - l)/l$, $\bar{x}_3 = (x_3 + l)/l$, and $\bar{y}_1 = y_1/l$; the length scale is set equal to equilibrium length l of the C–O interatomic length; $l = 1.16 \times 10^{-10}$ m)

$$\bar{H} = \bar{T} + \bar{\Pi}, \tag{1}$$

where

$$\bar{T} = \frac{1}{2}\{2\dot{\bar{\vartheta}}_1^2 + 2M_2\dot{\bar{\vartheta}}_2^2 + 2M_2\dot{\bar{\vartheta}}_3^2\}, \tag{2}$$

is the kinetic energy and

$$\begin{aligned}\bar{\Pi} = \frac{1}{2}\Bigg\{&\sigma^2[K_{CO}(\Delta\bar{r}_{12}^2 + \Delta\bar{r}_{23}^2) + 2K_{OO}\Delta\bar{r}_{12}\Delta\bar{r}_{23}] \\ &+ \frac{1}{2M_2}K_{\varphi\varphi}\Delta\varphi^2\Bigg\} + \frac{1}{6m_E}\{l^3[k_{rrr}(\Delta\bar{r}_{12}^3 + \Delta\bar{r}_{23}^3) \\ &+ 3k_{rrr'}\Delta\bar{r}_{12}\Delta\bar{r}_{23}(\Delta\bar{r}_{12} + \Delta\bar{r}_{23}) \\ &+ 3lk_{r\varphi\varphi}(\Delta\bar{r}_{23} - \Delta\bar{r}_{12})\Delta\varphi^2\} + \frac{1}{24m_E}\{l^4[k_{rrrr}(\Delta\bar{r}_{12}^4 + \Delta\bar{r}_{23}^4) \\ &+ 4k_{rrrr'}\Delta\bar{r}_{12}\Delta\bar{r}_{23}(\Delta\bar{r}_{12}^2 + \Delta\bar{r}_{23}^2) + 6k_{rrr'r'}\Delta\bar{r}_{12}^2\Delta\bar{r}_{23}^2] \\ &+ 6l^2[k_{rr\varphi\varphi}(\Delta\bar{r}_{12}^2 + \Delta\bar{r}_{23}^2) \\ &+ 2k_{rr'\varphi\varphi}\Delta\bar{r}_{12}\Delta\bar{r}_{23}]\Delta\varphi^2 + k_{\varphi\varphi\varphi\varphi}\Delta\varphi^4\}\end{aligned} \tag{3}$$

is the potential energy. In the above expressions, $\Delta\bar{r}_{12} = (\bar{r}_{12} - 1)$ and $\Delta\bar{r}_{23} = (\bar{r}_{23} - 1)$ are the elongations of mechanical couplings, $\bar{r}_{ij} = \sqrt{\bar{X}_{ij}^2 + \bar{Y}^2}$ is the distance between the ith and jth atoms ($\bar{X}_{12} = -\bar{\vartheta}_1 + M_2\bar{\vartheta}_3 - 1$, $\bar{X}_{23} = -\bar{\vartheta}_1 + M_2\bar{\vartheta}_3 + 1$, $\bar{Y} = M_2\bar{\vartheta}_2$), and $\Delta\varphi = \arctan(\bar{Y}/\bar{X}_{12}) - \arctan(\bar{Y}/\bar{X}_{23})$ is the change in the valence angle due to deformation vibrations. The parameters that are absent in [3] are as follows: k_{CO} and k_{OO} are the elongation-independent components of the stiffness of the springs that simulate C–O and O–O interatomic interactions, respectively; $k_{\varphi\varphi}$ is the invariable part of the flexural stiffness of the molecule; $K_{CO} = k_{CO}/k_q$, $K_{OO} = k_{OO}/k_q$, and $K_{\varphi\varphi} = k_{\varphi\varphi}/k_\varphi$ are the ratios of the above quantities to the coefficients of model [3], which were defined in [2] according to [4]; k_{rrr}, $k_{rrr'}$, $k_{r\varphi\varphi}$, k_{rrrr}, $k_{rrrr'}$, $k_{rrr'r'}$, $k_{rr\varphi\varphi}$, $k_{rr'\varphi\varphi}$, and $k_{\varphi\varphi\varphi\varphi}$ are other expansion coefficients, which were so designated (except for k and angle φ) in review [6] according to [5] and adopted (as well as k_{CO}, k_{OO}, and $k_{\varphi\varphi}$) in accordance with experimental data in [5], and $m_E = k_q l^2/\sigma^2$ is the energy scale. Overbarred quantities in expansion (3) of the potential, which are lacking in [3], characterize the physical anharmonicity of the vibrations.

It follows from the force versus the elongation characteristic dependence (Fig. 2) that the effects of anharmonicity arise when the deformation of interatomic bonds exceed 0.2.

Since the straggling of experimental data [6] for the coefficients at terms in the fourth power in expansion (3) is rather large, we will subsequently take into account only the cubed quantities in the expression for the potential (except for chaotic vibrations). It should also be noted that the farthest neighbor interaction (O–O interaction), the main part of which is taken into account through coefficient $K_{OO} = k_{OO}/k_q = 7.3 \times 10^{-2}$, is weak.

Having numerically solved the equations of motion written as the Lagrange equations of the second kind, which, up to deformation squared, have the form

$$\begin{aligned}&\ddot{\bar{\vartheta}}_1 + \frac{\sigma^2}{2}[-K_{CO}\bar{\xi}_{123,1}^- + K_{OO}\bar{\xi}_{231.1}^-] + \frac{\bar{Y}\bar{r}_{D123.2}^+\Delta\varphi}{4M_2} \\ &\quad + \frac{\sigma^2}{4}\{-K_{rrr}\bar{\xi}_{123,2}^- + K_{rrr'}\bar{R}^- + K_{r\varphi\varphi}\bar{\Phi}^+\} = 0, \\ &\ddot{\bar{\vartheta}}_2 + \frac{\sigma^2}{2}(K_{CO}\bar{D}_{r123.1}^+ + K_{OO}\bar{D}_{r231.1}^+)\bar{Y} + \frac{\bar{X}_{r123.2}^-\Delta\varphi}{4M_2} \\ &\quad + \frac{\sigma^2}{4}\{K_{rrr}\bar{D}_{r123,2}^+\bar{Y} + K_{rrr'}\bar{R}_{\bar{Y}} + K_{r\varphi\varphi}\bar{\Phi}_{\bar{Y}}\} = 0, \\ &\ddot{\bar{\vartheta}}_3 + \frac{\sigma^2}{2}[K_{CO}\bar{\xi}_{123.1}^+ + K_{OO}\bar{\xi}_{231.1}^+] - \frac{\bar{Y} - \bar{r}_{D123.2}^-\Delta\varphi}{4M_2} \\ &\quad + \frac{\sigma^2}{4}\{K_{rrr}\bar{\xi}_{123.2}^+ + K_{rrr'}\bar{R}^+ - K_{r\varphi\varphi}\bar{\Phi}^-\} = 0,\end{aligned} \tag{4}$$

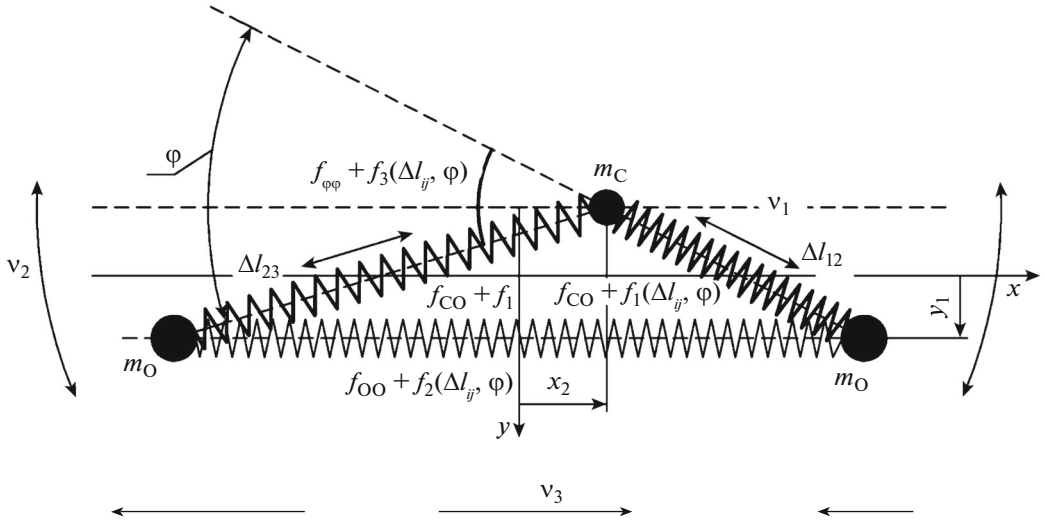

Fig. 1. Computational scheme.

where

$$\bar{\xi}^{\pm}_{123,p} = \bar{X}_{r,12}\Delta\bar{r}^{p}_{12} \pm \bar{X}_{r,23}\Delta\bar{r}^{p}_{23},$$

$$\bar{R}^{\pm} = \bar{X}_{r,23}\Delta\bar{r}^{\,2}_{12} \pm 2\bar{X}^{\pm}_{r123.1}\Delta\bar{r}_{12}\Delta\bar{r}_{23} \pm \bar{X}_{r,12}\Delta\bar{r}^{2}_{23},$$

$$\bar{R}_{\bar{Y}} = \Delta\bar{r}^{2}_{12}/\bar{r}_{23} + 2\bar{r}^{+}_{D123.1}\Delta\bar{r}_{12}\Delta\bar{r}_{23} + \Delta\bar{r}^{2}_{23}/\bar{r}_{12},$$

$$\bar{\Phi}^{\pm} = \bar{X}^{\pm}_{r123.1}\Delta\varphi^{2} + 2\bar{Y}\bar{r}^{\pm}_{D123.2}(\Delta\bar{r}_{23} - \Delta\bar{r}_{12})\Delta\varphi,$$

$$\bar{\Phi}_{\bar{Y}} = 2\bar{X}^{-}_{r123.2}(\Delta\bar{r}_{23} - \Delta\bar{r}_{12})\Delta\varphi - \bar{Y}\bar{r}_{D123.1}\Delta\varphi^{2},$$

$$\bar{\xi}^{\pm}_{231,p} = \bar{X}_{r,23}\Delta\bar{r}^{p}_{12} \pm \bar{X}_{r,12}\Delta\bar{r}^{p}_{23},$$

$$\bar{X}_{r,ij} = \bar{X}_{ij}/\bar{r}_{ij},$$

$$\bar{r}^{+}_{D123,p} = 1/\bar{r}^{p}_{12} \pm 1/\bar{r}^{p}_{23},$$

$$\bar{X}^{\pm}_{r123.1} = \bar{X}_{12}/\bar{r}^{p}_{12} \pm \bar{X}_{23}/\bar{r}^{p}_{23},$$

$$\bar{D}^{\pm}_{r123,p} = \Delta\bar{r}^{p}_{12}/\Delta\bar{r}_{12} \pm \Delta\bar{r}^{p}_{23}/\bar{r}_{23},$$

$$\bar{D}^{\pm}_{r231,p} = \Delta\bar{r}^{p}_{12}/\bar{r}_{23} \pm \Delta\bar{r}^{p}_{23}/\bar{r}_{12},$$

$$K_{rrr} = k_{rrr}/(k_q/l),$$

$$K_{rrr'} = k_{rrr'}/(k_q/l),$$

$$K_{r\varphi\varphi} = k_{r\varphi\varphi}/(k_q l) \quad (p \in Z, \text{Fig. 3}),$$

one can draw the following conclusions.

(i) The physical nonlinearity changes the motion picture neither quantitatively nor qualitatively. Therefore, nonlinearity should be taken into account only for refining the intensity of weak lines viewed as solution harmonics. (see Section 3).

(ii) In the case of small-amplitude vibrations and the initial conditions that provide the maximal rate of energy exchange between degrees of freedom, symmetric $\vartheta_1(t)$ vibrations and deformation $\vartheta_2(t)$ vibrations do not excite antisymmetric $\vartheta_3(t)$ vibrations. Therefore, in our case, we can have $\{\bar{\vartheta}_{20} \ll \bar{\vartheta}_{10}, \bar{\vartheta}_{10} \ll 1\}$ $\bar{\vartheta}_{30} = 0$ and $\dot{\bar{\vartheta}}_{30} = 0$ and disregard antisymmetric vibrations when seeking an approximate analytic solution.

For detailed analysis, let us consider the dependence of the maximal absolute deviation along the antisymmetric coordinate ($\max|\bar{\vartheta}_3|$) from $\bar{\vartheta}_{10}$. The

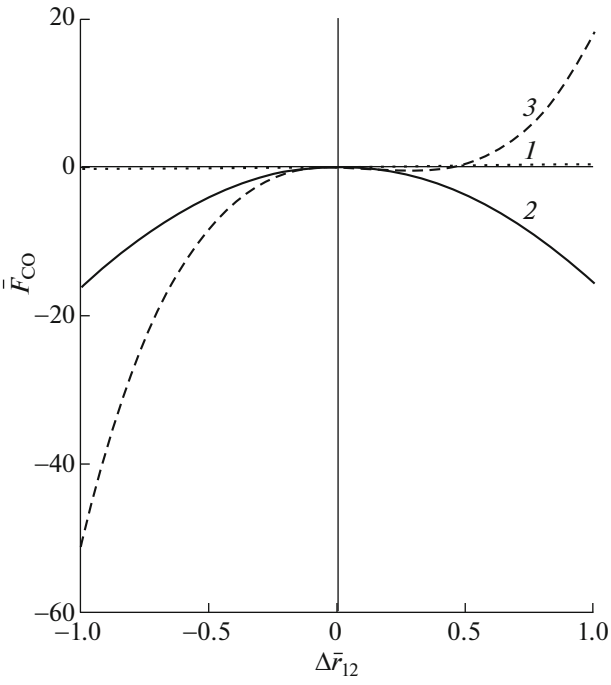

Fig. 2. Elastic characteristic of C–O bonds: (*1*) linear approximation (Hooke's law), (*2*) quadratic approximation, and (*3*) cubic approximation.

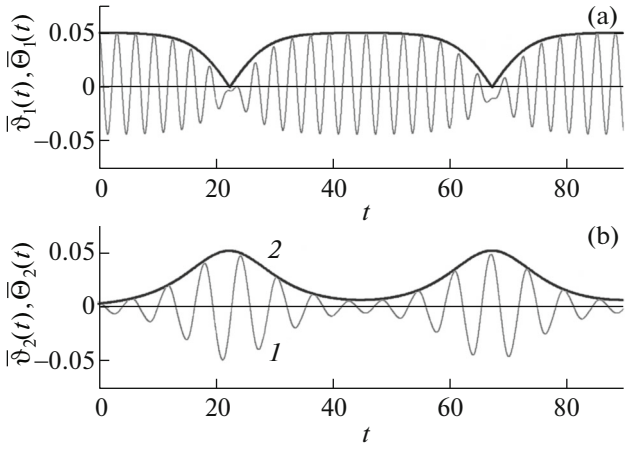

Fig. 3. (*1*) Numerical solution of Eq. (4) vs. its analytical solution in the first approximation (curves *2* are the envelopes given by (7)).

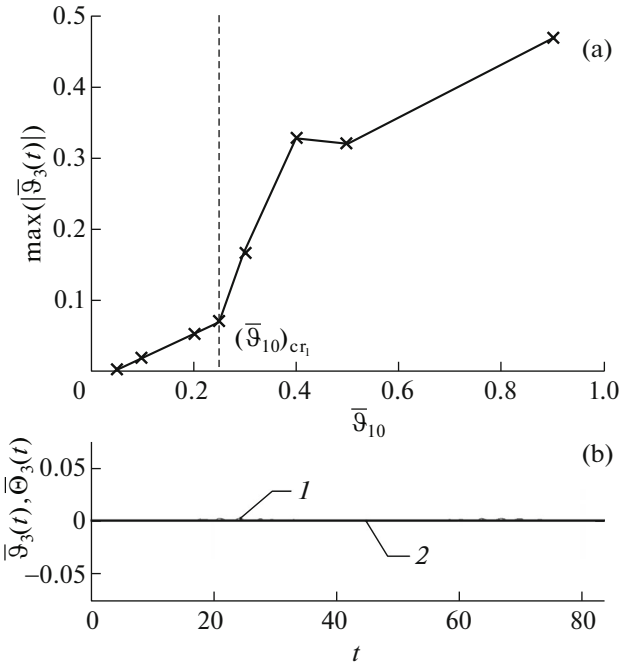

Fig. 4. Excitation of antisymmetric vibrations under the combined action of symmetric and deformation initial deviations: (a) $\max(|\overline{\vartheta}_3(t)|)$ vs. $\overline{\vartheta}_{10}$ and (b) oscillatory process (numerical simulation) under the conditions of Fig. 3: (*1*) calculated curve and (*2*) envelope (7).

splitting of spectral lines is most distinctly seen in the asymptotic case; therefore, a solution will be sought for initial conditions $\overline{\vartheta}_{20} \ll \overline{\vartheta}_{10}$ and $\overline{\vartheta}_{30} = 0$. Quantity $\overline{\vartheta}_{10}$ is varied, that ratio $\overline{\vartheta}_{10}/\overline{\vartheta}_{20}$ is kept equal to 10. Analytical results (Fig. 4) show that $\overline{\vartheta}_{10}$ has a critical value $(\overline{\vartheta}_{10})_{cr} \approx 0.25$), above which $\overline{\vartheta}_3$ has a significant influence on the Fermi resonance.

It can be shown that an antisymmetric perturbation influences the symmetric and flexural (deformation) motion of the molecule in the same way. Based on the curves depicted in Fig. 5a, one can predict the stability of symmetric and deformation vibrations of the molecule against antisymmetric initial deviation $\overline{\vartheta}_{30}$ (all initial momenta are taken to be zero). The critical value of $\overline{\vartheta}_{30}$ can be seen to obviously correlate with $(\overline{\vartheta}_{10})_{cr}$ shown in Fig. 4; their ratio is roughly equal to ratio $\overline{\vartheta}_{20}/\overline{\vartheta}_{10}$ taken at the previous stage of simulation (simulation data are shown in Fig. 4). If the amplitudes of vibrations along the $\overline{\vartheta}_{30}$ coordinate are small, the energy exchange between the symmetric and antisymmetric forms is weak (Fig. 5b; cf., Fig. 4b, in which the envelope of the solution is shown in the first approximation $\overline{\Theta}_3(t) = \overline{\vartheta}_{30}$. The envelope will be derived in the next section using the equivalent normal form method combined with the invariant normalization algorithm [7]). Under the given initial conditions, vibrations take place along the axis of the undeformed molecule and flexural vibrations with frequency ν_2 are not excited. However, the deformation vibrations may be unstable, as a result of which even a small initial deviation $\overline{\vartheta}_{20}$ may build them up.

Fermi [4], as well as the authors of this work [3, 8], believed that antisymmetric vibrations do not affect interaction between symmetric and deformation vibrations. The above results allow us to determine the applicability conditions for the classical approach, including small-amplitude vibrations, in which case the motion is regular.

2. ASYMPTOTIC ANALYSIS OF ENERGY EXCHANGE BETWEEN DEGREES OF FREEDOM

Let us reduce the method of reducing a set of equations to the Poincaré–Birkhoff recurrence normal form using the invariant normalization algorithm in the Zhuravlev–Petrov form [7]. Normalizing Hamiltonian (1), we can reduce it to the integrable form [3]

$$\frac{m_t^2}{m_H} = \bar{H} = \bar{H}_2 + \bar{H}_3$$
$$= \frac{1}{2}\{[\overline{\psi}_1^2 + 4\overline{q}_1^2] + [\overline{\psi}_2^2 + \tilde{\tilde{\Omega}}_2^2\overline{q}_2^2] + [\overline{\psi}_3^2 + \tilde{\tilde{\Omega}}_3^2\overline{q}_3^2]\} \quad (5)$$
$$+ \tilde{k}_{111}q_1^3 + \frac{3}{2}\overline{q}_1\overline{q}_2^2 + \tilde{k}_{133}\overline{q}_1\overline{q}_3^2 + \tilde{k}_{322}\overline{q}_3\overline{q}_2^2 + \tilde{\mu}\overline{q}_1^2.$$

Here, $\tilde{t} = t/m_{\tilde{t}}$ is the normalized time; $\overline{q}_j = \overline{\vartheta}_j/m_j$ and $\overline{\psi}_j = \mathrm{dot}\overline{q}_j = d\overline{q}_j/d\tilde{t}$ ($j = 1$–3) are the normalized coordinates and velocities; $m_{\tilde{t}} = 1/\sqrt{K_{CO} + K_{OO}} = 0.990$, $m_1 = S$, $m_2 = m_3 = S/\sqrt{M_2}$, and $m_H = 2S^2$ are the normalization factors for the time, coordinates, and Hamiltonian, respectively ($S = 3M_2(K_{CO} + K_{OO})/k_{122}$);

$\tilde{k}_{111} = (m_{\tilde{i}}^2 m_1^3/m_H)k_{111}$; $\tilde{k}_{113} = (m_{\tilde{i}}^2 m_1 m_3^2/m_H)k_{133}$; $\tilde{k}_{322} = (m_{\tilde{i}}^2 m_3 m_2^2/m_H)k_{322}$; $\tilde{\mu} = 4(K_{CO} + K_{OO})(m_{\tilde{i}} m_1^2/m_H)\mu$; $k_{111} = \sigma^2/3(k_{rrr} + 3k_{rrr'})l/k_q < 0$; $k_{122} = \sigma^2 M_2^2\,[(K_{CO} + K_{OO}) - 2/M_2 K_{\varphi\varphi} + 2/300(lk_{rrr}/k_q)] > 0$ (that is, coefficients $k_{r\varphi\varphi}$ of the expansion in the physical nonlinearity parameters, despite their analogy with the coefficient at $\bar{q}_1\bar{q}_2^2$ in expansion (5) in the physical nonlinearity parameters in the cubic part of the potential, do not influence the parameters of energy exchange between modes),

$$k_{133} = \sigma^2 M_2^2 l(k_{rrr} - k_{rrr'})/k_q < 0.$$

$$\begin{aligned} k_{322} &= 4\sigma^2 M_2^3(k_{r\varphi\varphi}/k_{ql}) \\ &= 4\sigma^2 M_2^3\{k_{r\varphi\varphi}/[(2M_2\sigma^2/t^2)k_\varphi l]\} \\ &= 2M_2^2(lk_{r\varphi\varphi}/k_\varphi) < 0. \end{aligned}$$

Indeed, up to deformation terms cubed in (3), springs that model interatomic interactions are soft and physical anharmonicity has a minor influence on coefficient k_{122} at the resonance term. This coefficient is responsible for energy exchange between modes. The time is normalized for taking into account the deviation of the total relative constant part of the stiffness coefficient for C–O and O–O bonds from unity due to extension–tension, $K_{CO} + K_{OO} = 1.020$. In (1), the time is not normalized in order to show the influence of different components of stiffness (k_{CO}, k_{OO}, $k_{\varphi\varphi}$) on the oscillation frequency of the linearized system. The fundamental oscillation frequencies of the linearized system will be $\tilde{\bar{\Omega}}_1 = \bar{\Omega}_1/m_{\tilde{\omega}} = \bar{\Omega}_1 m_{\tilde{i}} = \sigma = 2 + \mu$, $\tilde{\bar{\Omega}}_1 = \bar{\Omega}_2 m_{\tilde{i}} = \sqrt{K_{\varphi\varphi}} m_{\tilde{i}} = 1.005 \times 0.990 = 0.99 \approx 1$, and $\tilde{\bar{\Omega}}_3 = \bar{\Omega}_3 m_{\tilde{i}} = (K_{CO} - K_{OO})\sqrt{11/3}\ (2 + \mu) m_{\tilde{i}} \approx 2\sqrt{11/3} \approx 4$, respectively. The frequency detuning in the form $(\tilde{\bar{\Omega}}_1/\tilde{\bar{\Omega}}_2 - 2)$ is not introduced in order to prevent the escape of experimental errors [5] into frequencies $\nu_1 = 1338\ \text{cm}^{-1}$ and $\nu_2 = 667\ \text{cm}^{-1}$ [2].

To take into account the offset of frequencies ν_1 and ν_2 from integer ratio 2 : 1, $\mu = \sigma - 2 = \nu_1/\nu_2 - 2$, one can, as in [8] (the cubic part of Hamiltonian $\bar{H}_3$ is similar to that presented in [8], and terms containing $\bar{q}_1^3$, $\bar{q}_1\bar{q}_3^2$, and $\bar{q}_3\bar{q}_2^2$, which is lacking in [3, 8], do not influence the normal form of the first approximation), see an analogy with [9]. This results in an asymptotic solution within the interval ($t \in [0; nT]$ (for initial deviations $\bar{\vartheta}_{10} = 0.05$ and $\bar{\vartheta}_{20} = 0.1\bar{\vartheta}_{10}$ and zero initial momenta, the period of energy exchange (transfer [7, 9]) between the symmetric and deformation degrees of freedom is $T = 44.612$) in the form of a sum of n solitons:

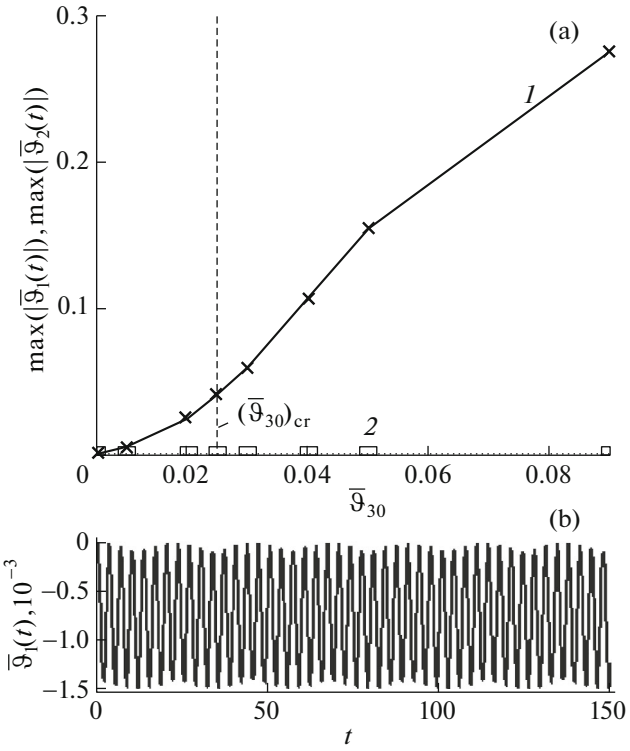

Fig. 5. Excitation of symmetric and deformation vibrations by an antisymmetric initial deviation: (a) (*1*) $\max(|\bar{\vartheta}_1(t)|)$ and (*2*) $\max(|\bar{\vartheta}_2(t)|)$ vs. $\bar{\vartheta}_{30}$ ($\bar{\vartheta}_{10} = \bar{\vartheta}_{20} = 0$) and (b) oscillatory process (numerical simulation) under the initial conditions $\bar{\vartheta}_{30} = 5 \times 10^{-3}$, $\bar{\vartheta}_{j0} = 0$, $\dot{\bar{\vartheta}}_{n0} = 0$ ($j = 1, 2$; $n = 1$–3).

$$\begin{gathered} \bar{\vartheta}_{1a}(t) = \bar{\Theta}_1(t)\cos 2t, \quad \bar{\vartheta}_{2a}(t) = \bar{\Theta}_2(t)\cos t, \\ \bar{\vartheta}_{3a}(t) = \bar{\Theta}_3(t)\cos\bar{\Omega}_3 t, \end{gathered} \tag{6}$$

$$\bar{\Theta}_1(t) = \bar{\vartheta}_{10}\left\{\sum_{i=1}^{n}\left|\tanh\left[\tau(t) - (1 + 2(i-1))\frac{\tau_0}{2}\right]\right| - (n-1)\right\},$$

$$\bar{\Theta}_2(t) = \frac{2}{\sqrt{M_2}}\bar{\vartheta}_{10}\sum_{i=1}^{n}\operatorname{sech}\left[\tau(t) - (1 + 2(i-1))\frac{\tau_0}{2}\right], \tag{7}$$

$$\bar{\Theta}_3(t) = \bar{\vartheta}_{30}.$$

As follows from the basic relationships of the normal form algorithm [7], the first approximation does not contain the antisymmetric oscillation exactly because its frequency considerably differs from the other two frequencies, which are responsible for the third-order internal resonance (as was noted as early as in 1931 by Fermi [4]). It should be noted that analytical solution (6) agrees well with the numerical solution (Fig. 3): the beating periods of the numerical solution along coordinates $\bar{\vartheta}_1$ and $\bar{\vartheta}_2$ are $T_1 = 44.903$ and $T_2 = 44.573$, respectively, and the arithmetic mean of the periods equals $T_{12m} = (T_1 + T_2)/2 = 44.\,738$. By virtue of the energy conservation law, the equality $T_1 = T_2 =$

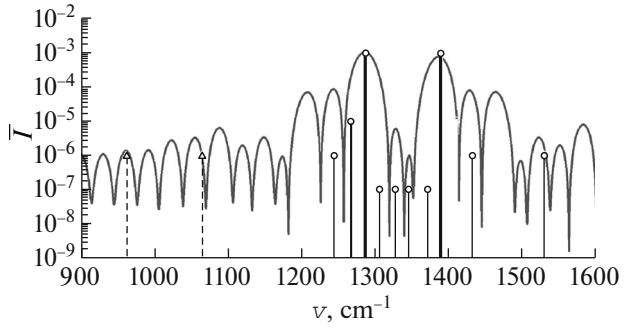

Fig. 6. Spectrum of the numerical solution to the complete equations in the neighborhood of symmetric vibration frequency ν_1 under the initial conditions that correspond to Fig. 3.

T must be fulfilled. The difference $(T_1 - T_2)$ is much smaller than T_1 and T_2, which indicates a

high calculation accuracy. A number of differences seem to be associated with the introduction of offsets into spectroscopic data [2] (the antisymmetric coordinate interacting, according to Figs. 4b and 4c, with the symmetric and deformation ones is embodied in the term $[l^3/(6m_E)]k_{rrr}(\Delta\bar{r}_{12}^3 + \Delta\bar{r}_{23}^3)$ of the potential (3); in contrast to [8], the cubic nonlinearity of the spring deformation influences the energy exchange period (the absence of the lateral displacement of the corresponding initial conditions is disregarded)). This point calls for further investigation.

3. SPECTRAL ANALYSIS

When the energy transfer between the degrees of freedom is the most intense, the solution to the governing equations corresponding to Hamiltonian (1) (both numerical equation and analytical equation (6)) is periodic. Therefore, it can be expanded into a Fourier series. Harmonics, the frequencies of which differ little from the fundamental frequency, make the greatest contribution to the sum.

The thus obtained spectrum of the harmonic intensities of symmetric oscillation $\bar{\vartheta}_1(t)$ is shown in Fig. 6. When imposed on experimental lines [2] (the dimensionless intensities of these lines were classified based on a qualitative criterion: intense, medium-intensity, weak, and very weak. Continuous and dashed vertical lines in Fig. 6 show combination and IR spectral lines, respectively. The thickness and height of the vertical lines correlate with their dimensionless intensity), and the spectrum makes it possible to identify a greater number of frequencies compared with linear [3] and quadratic [8] approximations as applied to elastic forces.

4. IRREGULAR MODES OF MOTION

It is known that the presence of two or more positions of stable equilibrium separated by unstable positions or potential barriers in a dynamic system may cause chaotic induced vibrations, which, in turn, may result in hops between neighboring equilibrium positions [10]. In systems with many degrees of freedom, the role of external loads for a given normal coordinate is played by other coordinates; therefore, the above scenario is also possible under noninteraction conditions.

In accordance with the aforesaid, antisymmetric oscillation $\bar{\vartheta}_3$ is disregarded. It does not influence [3, 8] the parameters of regular energy exchange between the degrees of freedom of the molecule (the question of whether it influences chaotic vibrations calls for further investigation). Then, it becomes possible to plot potential (3) in the space of two arguments, $\bar{\vartheta}_1$ and $\bar{\vartheta}_2$ (Fig. 7).

It follows from this plot that taking into account additional (compared with the physically linear model [3, 11]) anharmonicity has a minor effect on the position of the saddle point, but it does reflect the maximum of the potential. Consequently, the influence of new anharmonic frequencies is expected to show up in the neighborhood of the saddle point. For this reason, fourth-order terms in expansion (3) were ignored in the case of small-amplitude vibrations (Figs. 3, 4 at $\bar{\vartheta}_{10} \le 0.2$; Fig. 5 at $\bar{\vartheta}_{30} \le 0.02$; Fig. 6). As has been noted in Section 1, the accuracy of the experimental analysis of these vibrations (data [6]) is not high.

Expanding potential $\bar{\Pi}_{12} = \bar{\Pi}_{12}(\bar{\vartheta}_1, \bar{\vartheta}_2)$ into a series and discarding fourth-order terms, we obtain

$$\bar{\Pi}_{12}(\bar{\vartheta}_1, \bar{\vartheta}_2) = \bar{\Omega}_1^2\bar{\vartheta}_1^2 + M_2\bar{\Omega}_2^2\bar{\vartheta}_2^2 + k_{111}\bar{\vartheta}_1^3 + k_{122}\bar{\vartheta}_1\bar{\vartheta}_2^2 + k_{1111}\bar{\vartheta}_1^4 + k_{1122}\bar{\vartheta}_1^2\bar{\vartheta}_2^2 + k_{2222}\bar{\vartheta}_2^4 + o(\varepsilon^5), \quad (8)$$

where

$$k_{1111} = (\sigma^2/12)[l^2(k_{rrrr} + 4k_{rrrr'} + 3k_{rrr'r'})/k_q] > 0,$$

$$k_{1122} = 2\sigma^2M_2^2[(k_{rr\varphi\varphi} + k_{rr'\varphi\varphi})/k_q] - \sigma^2M_2^2(K_{CO} + K_{OO}) + 3M_2K_{\varphi\varphi} + \sigma^2M_2^2/2[l(k_{rrr} + 3k_{rrr'})/k_q] < 0,$$

$$k_{2222} = (\sigma^2/4)M_2^4((K_{CO} + K_{OO}) - 2/3M_2^3K_{\varphi\varphi} + (2/3)\sigma^2M_2^4(k_{\varphi\varphi\varphi\varphi}/k_ql^2) > 0.$$

Small parameter ε is taken to be equal to unity.

Thus, two wells in potential $\bar{\Pi}_{12}$ $(\bar{\vartheta}_1, \bar{\vartheta}_2)$ approximated by (8) are due to only the term containing the product $\bar{\vartheta}_1^2\bar{\vartheta}_2^2$. If the Mel'nikov necessary condition [12, 13] for chaos is used (specifically, for determining the sizes of the chaotic domain in the phase space), it becomes impossible to take single-degree-of-freedom systems as undisturbed. This requirement follows from the well-known [14, 15] generalization of the

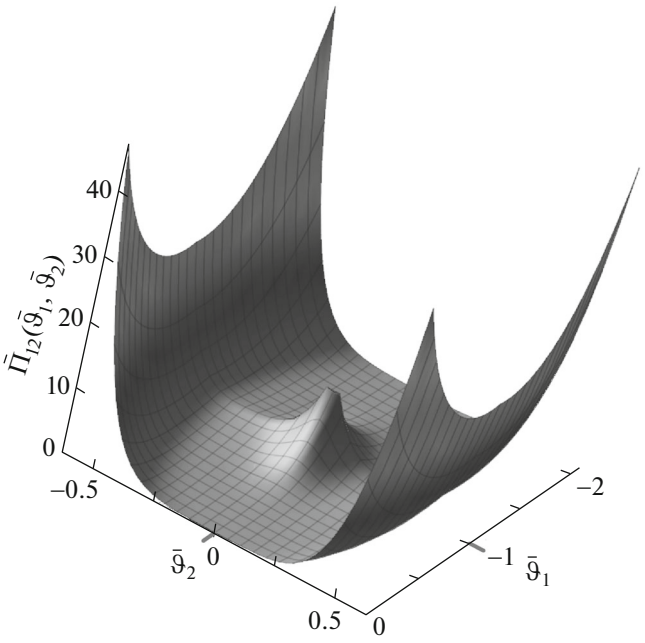

Fig. 7. Surface of the potential in the mechanical model of the molecule ($\bar{\Pi}_{12}(\bar{\vartheta}_1, \bar{\vartheta}_2) = \bar{\Pi}(\bar{\vartheta}_1, \bar{\vartheta}_2, \bar{\vartheta}_3 = 0)$).

Mel'nikov method for autonomous systems with many degrees of freedom.

Numerical simulation reveals a stochastic attractor in the system (Fig. 8).

If the initially stored energy is in accord with the potential energy at the saddle point, the interaction of the symmetric and deformation oscillation modes with the antisymmetric one is possible for any value of ratio $\bar{\vartheta}_{30}/\bar{\vartheta}_{10}$ and $\bar{\vartheta}_{20}$.

For example, antisymmetric vibrations may be excited by symmetric and deformation vibrations for $\bar{\vartheta}_{10}$ greater than its critical value $(\bar{\vartheta}_{10})_{cr}$ (Fig. 1). Figure 9a exemplifiers the typical dependence $\bar{\vartheta}_3(t)$ under the conditions described in the caption to Fig. 8 (the scales and the ranges of parameters are the same as in Fig. 3 for comparison), when a strange attractor arises in the system.

Similarly, antisymmetric vibrations may excite symmetric vibrations if $\bar{\vartheta}_{30} > (\bar{\vartheta}_{30})_{cr}$. This condition is sufficient for falling into the neighborhood of the saddle point (Fig. 9b).

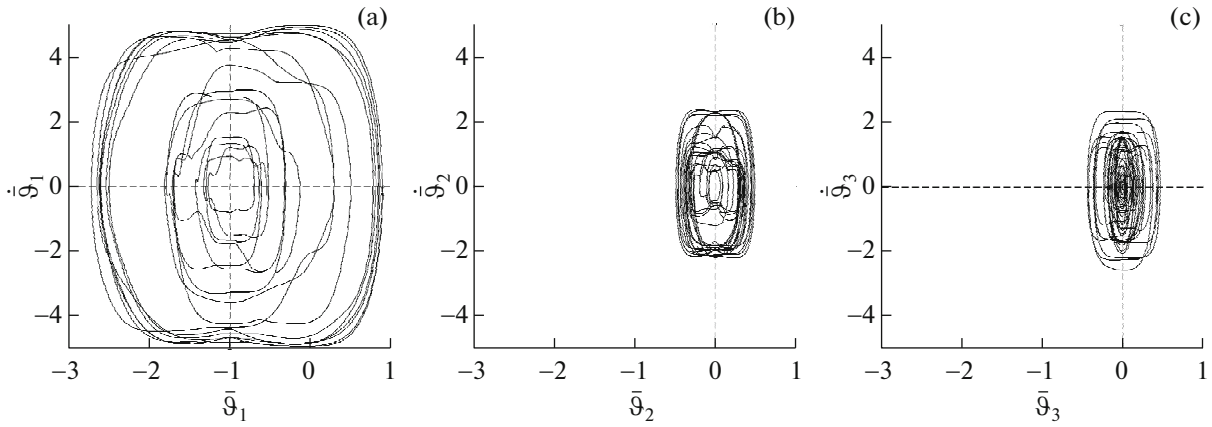

Fig. 8. Phase portraits of (a) symmetric vibration $\bar{\vartheta}_1$, (b) deformation vibration $\bar{\vartheta}_2$, and (c) antisymmetric vibration $\bar{\vartheta}_3$ under the initial conditions $\bar{\vartheta}_{10} = 0.9$, $\bar{\vartheta}_{20} = 0.09$, $\bar{\vartheta}_{30} = 0$, $\dot{\bar{\vartheta}}_{10} = 0$, $\dot{\bar{\vartheta}}_{20} = 0$, and $\dot{\bar{\vartheta}}_{30} = 0$.

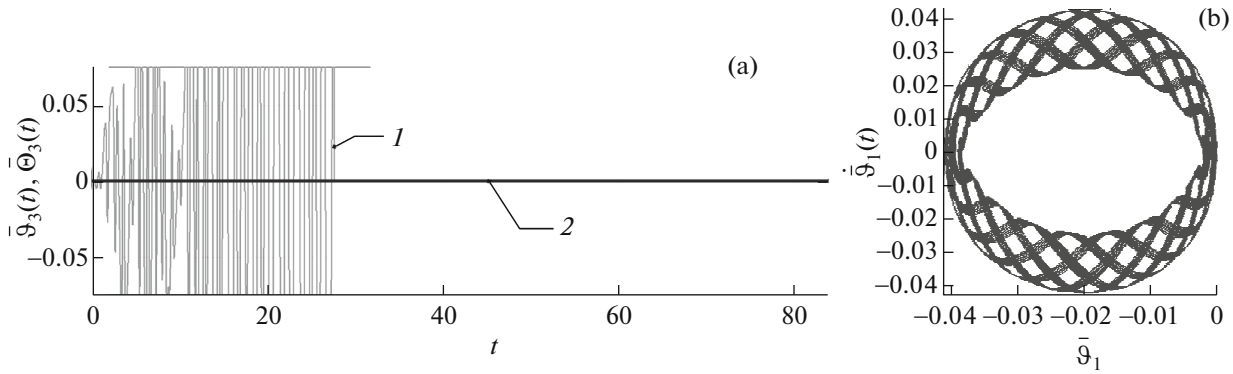

Fig. 9. Typical oscillatory process: (a) plot $\bar{\vartheta}_3(t)$ under the conditions of Fig. 8 (the count time equals 27 630 units of dimensionless time) and (b) phase portrait ($\bar{\vartheta}_{30} = 2.5 \times 10^{-2}$, $\bar{\vartheta}_{j0} = 0$, $\dot{\bar{\vartheta}}_{n0} = 0$ ($j = 1, 2$; $n = 1–3$)).

The rate of transition from regular to stochastic vibrations is a subject of separate consideration.

CONCLUSIONS

We suggested an approach to studying the nonlinear vibrations of a CO_2 molecule that is based on classical dynamics. Equations of molecule vibrations were derived in the farthest neighbor approximation, which includes the anharmonicity of valence vibrations and the force field of the molecule (the stiffness and softness of springs). The equations were solved both numerically and analytically using the invariant normalization method. It was found that the anharmonicity of deformation vibrations makes a major contribution to the Fermi resonance. Taking into account the anharmonicity of the force field and O–O bonds in the molecule makes it possible to determine additional frequencies in the spectrum of the molecule. A strange attractor was revealed by numerical simulation. Recommendations are given for selecting initial conditions for the excitation of vibrations in the molecule that prevent the regular vibrations from changing to chaotic vibrations.

REFERENCES

1. M. V. Vol'kenshtein, M. A. El'shevich, and B. I. Stepanov, *Oscillations of Molecules* (Gostekhizdat, Moscow, 1949).
2. G. Herzberg, *Infrared and Raman Spectra of Polyatomic Molecules* (Van Nostrand, New York, 1947; Izd. Inostr. Lit., Moscow, 1949).
3. G. T. Aldoshin and S. P. Yakovlev, Izv. Ross. Akad. Nauk, Mekh. Tverd. Tela, No. 32, 42 (2015).
4. E. Fermi, Z. Phys. **71**, 250 (1931).
5. M. Lacy, Mol. Phys. **45**, 253 (1982).
6. A. G. Csåszår, J. Phys. Chem. **96**, 7898 (1992).
7. A. G. Petrov, Izv. Ross. Akad. Nauk, Mekh. Tverd. Tela, No. 5, 18 (2006).
8. G. T. Aldoshin and S. P. Yakovlev, in *Proceedings of All-Russia Meeting on Fundamental Problems of Theoretical and Applied Mechanics, Kazan', 2015* (Izd. Kazansk. Federal. Univ., Kazan', 2015), pp. 109–111.
9. A. G. Petrov and A. M. Shunderyuk, Izv. Ross. Akad. Nauk, Mekh. Tverd. Tela, No. 2, 27 (2010).
10. G. T. Aldoshin, *Theory of Linear and Nonlinear Oscillations: A Student Book* (Lan', St. Petersburg, 2013).
11. G. T. Aldoshin and S. P. Yakovlev, in *Proceedings of the International Conference on Mechanics 7th Polyakhov's Readings, St. Petersburg, 2015,* pp. 1–4.
12. E. Simiu, *Chaotic Transitions in Deterministic and Stochastic Dynamical Systems. Applications of Melnikov Processes in Engineering, Physics, and Neuroscience* (Princeton Univ., Princeton, 2002; Fizmatlit, Moscow, 2007).
13. A. S. Ledkov, "*Investigation of resonant motion of segment-conical bodies in the atmosphere,*" Candidate's Dissertation (Samara, 2009).
14. L. M. Perko, Rocky Mt. J. Mat. **22**, 980 (1992).
15. J. E. Marsden and T. S. Ratiu, *Introduction to Mechanics and Symmetry: A Basic Exposition of Classical Mechanical Systems,* 2nd ed. (Springer, New York, 1998).

Translated by V. Isaakyan